ACS OMEGA

http://pubs.acs.org/journal/acsodf

Article

High-Throughput Exonuclease Assay Based on the Fluorescent Base Analogue 2-Aminopurine

Margherita M. Botto, Sudarshan Murthy, and Meindert H. Lamers*

Cite This: *ACS Omega* 2023, 8, 8285−8292

Read Online

ACCESS | Metrics & More | Article Recommendations | Supporting Information

ABSTRACT: Exonucleases are essential enzymes that remove nucleotides from free DNA ends during DNA replication, DNA repair, and telomere maintenance. Due to their essential role, they are potential targets for novel anticancer and antimicrobial drugs but have so far been little exploited. Here, we present a simple and versatile real-time exonuclease assay based on 2-aminopurine, an intrinsically fluorescent nucleotide that is quenched by neighboring bases when embedded in DNA. We show that our assay is applicable to different eukaryotic and bacterial exonucleases acting on both 3′ and 5′ DNA ends over a wide range of protein activities and suitable for a high-throughput inhibitor screening campaign. Using our assay, we discover a novel inhibitor of the *Mycobacterium tuberculosis* PHP-exonuclease that is part of the replicative DNA polymerase DnaE1. Hence, our novel assay will be a useful tool for high-throughput screening for novel exonuclease inhibitors that may interfere with DNA replication or DNA maintenance.

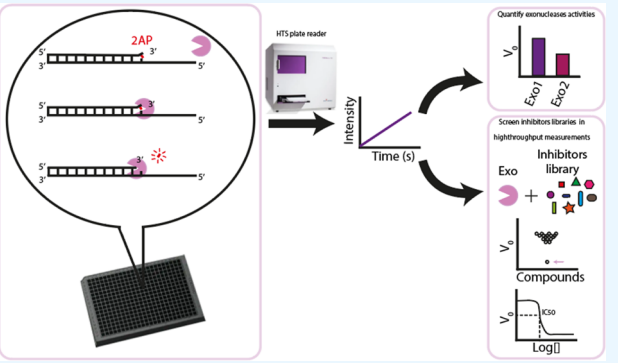

INTRODUCTION

Exonucleases are essential enzymes that remove mis-incorporated nucleotides during DNA replication, modify DNA during crosslink repair, mismatch repair, nonhomologous end-joining, and nucleotide excision repair and also during telomere maintenance (reviewed in ref 1). Exonucleases cleave the terminal nucleotide of either single- or double-stranded DNA and can act in either a 3′−5′ or a 5′−3′ direction. They are distinct from endonuclease that cut DNA internally. Because of their essential roles in DNA replication and DNA repair, they are potentially attractive targets for novel therapeutics that aim to interfere with DNA synthesis or DNA maintenance. However, exonucleases have thus far been little exploited, with the exception of a small number of examples, such as the exonuclease domain of the *Mycobacterium tuberculosis* replicative DNA polymerase DnaE1[2] or the exonuclease domain of the *Streptococcus pneumoniae* replicative DNA polymerase Pol C.[3]

To aid in the discovery of novel exonuclease inhibitors, a suitable assay is needed that can be used in a high-throughput manner, thus excluding widely used gel-based assays that are laborious and time-consuming. Several real-time, fluorescence-based exonuclease assays have been reported, but each of these presents different drawbacks that may obstruct the discovery of novel inhibitors. For example, 5′-*p*-nitrophenyl ester of TMP works well on the *Escherichia coli* exonuclease ε[4] but is not hydrolyzed by the exonuclease of the replicative DNA polymerase DnaE1 from *M. tuberculosis* (Figure S1). Other real-time exonuclease assays use DNA intercalating dyes that could affect the activity of the exonuclease such as in ref 5. The intercalating dye-based assay furthermore requires processive exonuclease activity, as the removal of a single nucleotide will not suffice to change the fluorescent signal (Figure S2). Finally, fluorescent dyes coupled to the end of the DNA substrate[6] or fluorescent dye-quencher pairs have also been used,[7] but here, the presence of a bulky chemical group may interfere with enzymatic activity.

In this work, we present a high-throughput exonuclease assay based on 2-aminopurine (2-AP), an intrinsically fluorescent analogue of adenine and guanine[8] (Figure 1A). The fluorescence of 2-AP is quenched by the presence of neighboring bases in the DNA[9,10] but is restored when released by an exonuclease (Figure 1B). 2-AP has been previously used to inquire about nucleic acid structure,[11−14] their dynamics[15−17] and enzyme activity, including exonuclease activity,[10,18,20] DNA polymerase activity,[19] base-flipping activity,[21], DNA bending,[22] and DNA base pairing[23] (extensively reviewed in ref 24).

Although its proven versatility, thus far, 2-AP has not been applied for the use of high-throughput inhibitor screening.

Received: October 12, 2022
Accepted: January 20, 2023
Published: February 20, 2023

https://doi.org/10.1021/acsomega.2c06577
ACS Omega 2023, 8, 8285−8292

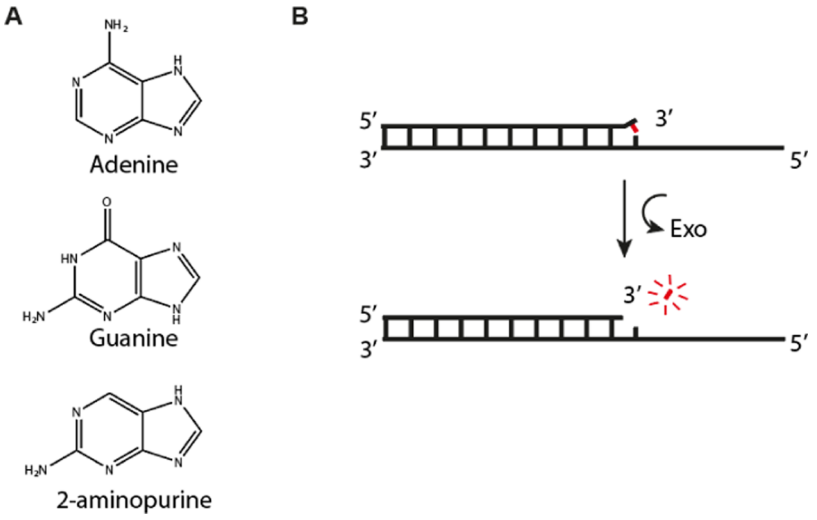

Figure 1. Principle of the 2-aminopurine exonuclease assay. (A) Comparison of the chemical structures of adenine, guanine, and 2-aminopurine. (B) Schematic representation of a DNA substrate containing a 2-AP nucleotide positioned at the 3′ end, where its fluorescence is quenched by the neighboring bases. Upon cleavage by an exonuclease, the 2-AP is released from the DNA, and its fluorescence is restored.

Here, we describe the use of 2-AP in an easy-to-use exonuclease assay suitable for high-throughput screening to measure exonuclease activity in real time. Due to its simplicity and minimal use of protein and substrate, this assay is suitable for screening of large chemical libraries to search for novel exonuclease inhibitors. We furthermore show an example where the 2-AP exonuclease assay is used to discover a new inhibitor of the exonuclease domain of the replicative DNA polymerase DnaE1 from *M. tuberculosis*.

MATERIALS AND METHODS

Chemicals and Reagents. All chemicals were purchased from Sigma unless indicated otherwise. DNA oligonucleotides were purchased from IDT. Chromatography columns were purchased from Cytiva.

Site-Directed Mutagenesis. Site direct mutagenesis was used to create the two active site mutants of the *E. coli* exonuclease ε. The methionine 18 to alanine (ε18) was created using the forward primer 5′-GAAACCACCGGTGCGAAC-CAGATTGGTGCG-3′ and reverse primer 5′-CGCAC-CAATCTGGTTCGCACCGGTGGTTTC-3.′ The valine 65 to alanine mutation (ε^{65}) was created using the forward 5′-GGAAGCCTTTGGCGCACATGGTATTGCCGATG-3′ and reverse primer 5′-CATCGGCAATACCATGTGCGC-CAAAGGCTTCC-3.′

Protein Expression and Purification. All proteins were expressed in *E. coli* BL21 (DE3) (Novagen) at 37 °C for 2 h unless otherwise stated. Protein purification was performed using buffer A (25 mM Imidazole pH 7.5, 500 mM NaCl, 2 mM DTT, 5% glycerol), buffer B (25 mM Tris pH 8.5, 2 mM DTT, 10% glycerol), buffer C (25 mM HEPES pH 7.5, 100 mM NaCl, 2 mM DTT), and buffer D (25 mM Tris pH 8.5, 2 mM DTT, 10% glycerol) with addition of imidazole or NaCl, as indicated. All purified proteins were flash-frozen in liquid nitrogen and stored at −80 °C.

Since *E. coli* ε is expressed in the insoluble fraction, after cell lysis and centrifugation, the pellet was solubilized in buffer A with 6 M urea and centrifuged at 24 000*g*. The supernatant was injected onto a HisTrap column pre-equilibrated in buffer A with 6 M urea and eluted using a gradient to 500 mM Imidazole in buffer A with 6 M urea. The eluted protein was diluted to 0.5 mg/mL in 25 mM Tris, 3 M Urea, and 2 mM DTT and refolded by overnight dialysis to buffer B. The refolded protein was centrifuged at 24 000*g* and injected onto a HiTrap Q column pre-equilibrated in buffer B with 40 mM NaCl and eluted with a gradient to 1 M NaCl in buffer B.

E. coli Pol I and Pol IIIα were purified using a HisTrap column pre-equilibrated in buffer A and eluted using a gradient to 500 mM Imidazole in buffer A. The his-tag was removed by overnight digestion with PreScission Protease (Cytiva), buffer-exchanged to buffer A, and followed by a second HisTrap column to remove undigested protein. The flowthrough was injected onto a HiTrap Q column pre-equilibrated in buffer B with 150 mM NaCl and eluted with a gradient to 1 M NaCl in buffer B. Pol IIIα was further purified using a Superdex 200 size exclusion column pre-equilibrated in buffer C.

M. tuberculosis DnaE1 was expressed in *Mycobacterium smegmatis* cells at 37 °C for 72 h. It was purified using a HisTrap column pre-equilibrated in buffer A and eluted using a gradient to 500 mM Imidazole in buffer A. The his-tag was removed by overnight digestion with PreScission Protease (Cytiva), buffer-exchanged to buffer A, and followed by a Heparin column. Lastly, it was further purified using a Superdex 200 size exclusion column pre-equilibrated in buffer C.

The catalytic domain of human Exo1 was expressed in *E. coli* BL21 (DE3) overnight at 18 °C.[25] It was purified using a HisTrap column pre-equilibrated in Buffer C with 20 mM Imidazole and eluted using a gradient to 300 mM Imidazole. Then, it was further purified using a HiTrap Q column equilibrated in Buffer C and eluted with a gradient to 1 M NaCl in Buffer C.

E. coli exonuclease I and exonuclease III were purchased from New England Biolabs.

Fluorescence Intensity Experiments. Assays were performed using oligonucleotides in Table S1. Fluorescence emission data were collected using a PHERAstar FSX microplate reader. All of the substrates and the proteins were individually diluted in 50 mM HEPES pH 7.5, 100 mM potassium glutamate, 5 mM $MgCl_2$, and 0.5 mg/mL BSA unless otherwise stated. Reactions were started by adding protein to DNA in a Corning 384-well Low Volume Black

https://doi.org/10.1021/acsomega.2c06577
ACS Omega 2023, 8, 8285−8292

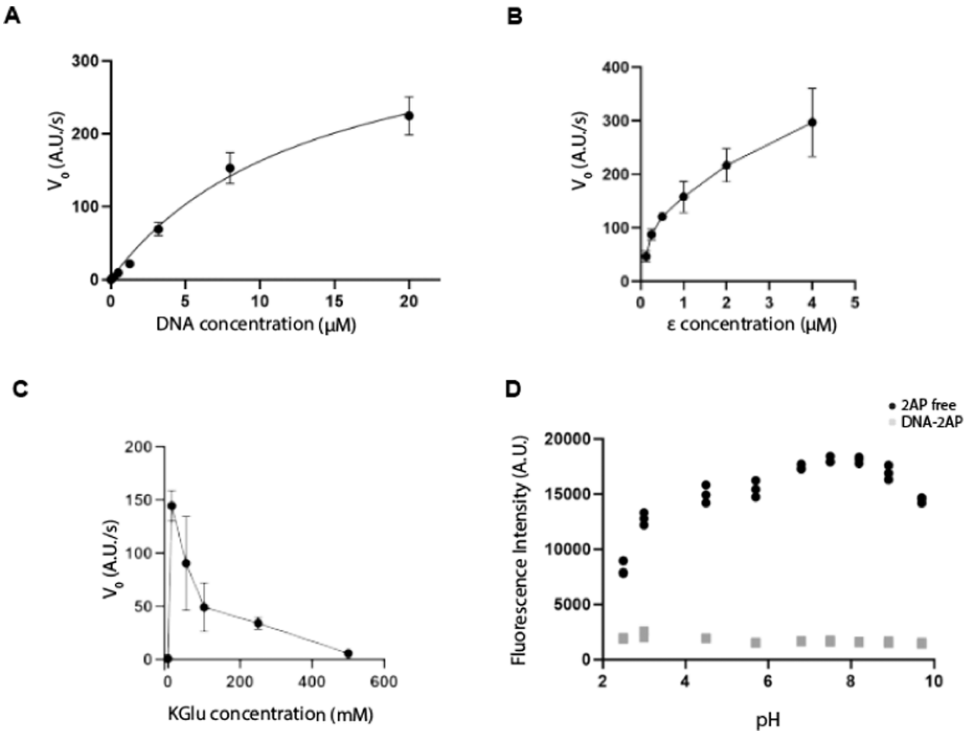

Figure 2. Determination of suitable working range for the 2-AP exonuclease assay. (A) Initial velocities (V_0) for the 2-AP exonuclease assay at 0.03−20 μM DNA and 0.5 nM *E. coli* ε exonuclease. Raw data shown in Figure S5. (B) Initial velocities (V_0) for the 2-AP exonuclease assay performed using 0.125−4 nM *E. coli* ε exonuclease and 0.5 μM DNA. Raw data are shown in Figure S6. (C) 2-AP exonuclease assay at 0−500 mM potassium glutamate (KGlu). Experiments performed using 0.5 μM DNA and 0.5 nM ε. (D) Difference between free 2-AP (black circles) and DNA-bound 2-AP (gray squares) over a pH range from 2.5 to 10. Buffers used are listed in Table S2. All data are derived from three or more independent experiments.

Round Bottom Polystyrene NBS Microplate (Corning #4514). Data were collected for 50 cycles, each lasting 20 s. All of the steps were performed at room temperature.

The samples were excited at 330 nm, and the emission was collected at 380 nm (for excitation and emission spectra, see Figure S3). A 320−380 filter (1904A1 BMG Labtech) was used to collect the measurements. To be able to compare measurements taken on different days with different exonucleases and on different substrates, all assays were performed using the same gain.

High-Throughput Screening Assays. For the high-throughput screening assays, we used the same oligonucleotides used for the manual assays (see Table S1). The oligonucleotides and protein (*M. tuberculosis* DnaE1) were diluted in 50 mM HEPES pH 7.5, 100 mM potassium glutamate, and 0.5 mg/mL BSA. Assays were dispensed using a Mantis liquid handler (Formulatrix) in 384-well polypropylene plates from Corning #4514. Data were collected for 30 cycles, each lasting for 60 s.

The assay validation statistics (Figure S4) were calculated using the following formulas:

$$\mathrm{S/B} = \frac{\text{mean signal}}{\text{mean background}}$$

$$\mathrm{S/N} = \frac{\text{mean signal} - \text{mean background}}{\text{standard deviation of background}}$$

where the mean signal is the fluorescent signal at completion of the assay in the presence of DNA and protein. The mean background is the negative control, where only DNA was added.

$$Z' = 1 - \frac{3(\text{SD of sample} + \text{SD of control})}{|\,\text{mean of sample} - \text{mean of control}\,|}$$

where "SD of sample" is the standard deviation of the positive control (DNA + protein) and the "SD of control" is the standard deviation of the negative control (DNA only).

Differential Scanning Fluorometry assays. The melting temperature of the *M. tuberculosis* DnaE1 was determined in the absence and presence of the ligand 6-thioinosine using a Tycho instrument (Nanotemper). Briefly, 8 μM of *M. tuberculosis* DnaE1 was incubated with 100 μM of 6-thioinosine for 10 min at 20 °C. Fluorescence intensity was followed at 330 and 350 nm while the temperature was increased from 35 to 95 °C over 3 min. Data were analyzed with Tycho software.

RESULTS

Optimization of Assay Conditions. To define a suitable working range for the 2-AP exonuclease assay, we analyzed the assay under different DNA, protein, and salt concentrations, as well as different pH values. For this, we used the *E. coli* exonuclease ε, a well-characterized enzyme responsible for the removal of mis-incorporated nucleotides during DNA replication.[26−29] Because the exonuclease ε works in a 3′ to 5′ direction, experiments were performed using a substrate containing a mismatched 2-AP at the 3′ end (substrate 2AP11 in Table S1). Using a range of DNA concentrations from 30 nM to 20 μM and a fixed amount of protein (0.5 nM), we

https://doi.org/10.1021/acsomega.2c06577
ACS Omega 2023, 8, 8285−8292

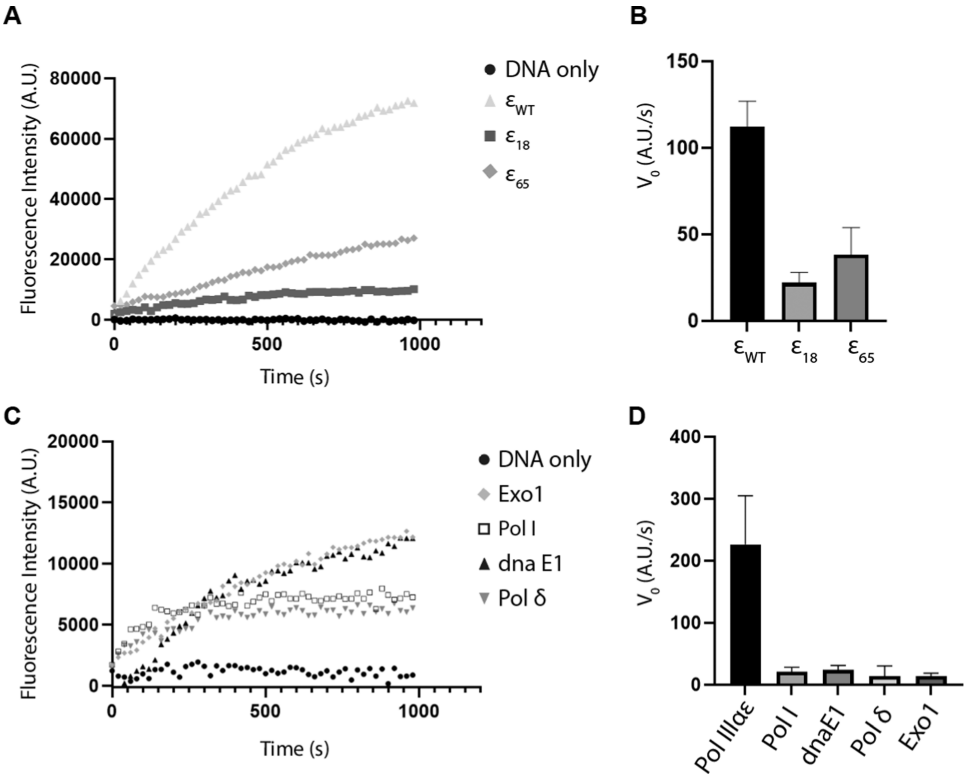

Figure 3. 2-AP exonuclease assay used on a variety of different proteins. (A) 2-AP exonuclease activity of wild-type ε and two active site mutants, ε^{18} and ε^{65}. Assays performed using 0.5 nM ε and 500 nM 2AP11 substrate. (B) Bar graph showing the initial velocity (V_0) for the curves shown in panel (A). (C) 2-AP exonuclease assay performed with *E. coli* Pol I, *M. tuberculosis* DnaE1, human Pol δ, and human Exo1. All proteins were used at 0.5 nM, except for Exo1, which was used at 10 μM. 500 nM of the substrate was used for all of the proteins. For Exo1 that is a 5′-3′ exonuclease, a DNA substrate with a 2-AP positioned at the 5′ was used (2AP11 reverse in Table S1). (D) Bar graph showing the initial velocity (V_0) for the curves shown in panel (C). For comparison, the V_0 of *E. coli* ε is included.

found a clear signal over the entire range, indicating the assay is sensitive over a wide range of substrate concentrations (Figure 2A). Therefore, to limit the amount of DNA consumed, we used 0.5 μM DNA in all subsequent assays. Next, we determined the enzyme working range by varying the concentration of ε from 0.125 to 4 nM (Figure 2B). Here too, we find that the assay gives a robust signal, even at concentrations as low as 0.125 nM. In addition, as salt can influence the interaction between many enzymes and DNA, we also varied the salt concentration while keeping the concentration of DNA and ε fixed at 0.5 μM and 0.5 nM, respectively (Figure 2C). Here, we find that for ε, there is an optimal salt concentration of ∼50 mM potassium glutamate, whereas no activity was observed at low (0 mM) or high (500 mM) salt concentrations. However, because the observed salt concentration for a bacterial cell is 100−200 mM, we decided to maintain a salt concentration of 100 mM for all subsequent experiments. Finally, as it has been reported that pH influences the fluorescence intensity of 2-AP,[30] we also measured the difference between free 2-AP and 2-AP incorporated into a DNA substrate over a wide range of pH values, from pH 2.5 to pH 10 (Figure 2D and Table S2). We find that the 8−9-fold difference between free 2-AP and DNA-bound remains stable between pH 5 and pH 10 and only drops to a 4-fold difference at pH 2.5. Hence, the assay is also applicable over a wide range of pH values.

Versatility of the Assay across Different Exonucleases Families. To further test the usefulness of the 2-AP exonuclease assay, we measured the activity of two *E. coli* ε mutants, ε18 and ε^{65}, alongside that of wild-type ε (Figure 3A,B). Both exonuclease mutants contain a mutation positioned at the entrance of the active site and have been shown to reduce exonuclease activity.[31] As anticipated, the two mutants ε18 and ε^{65} show a reduction in activity by 80 and 66%, respectively, indicating that the 2-AP assay is useful for the characterization of different mutant versions of a protein.

To further explore the versatility of the assay, we tested different 3′-5′ exonucleases from different organisms as well as a 5′−3′ exonuclease. For this, we used *E. coli* Pol I, *M. tuberculosis* DnaE1, human Pol δ holoenzyme (P125, p66, p50, p12), and the human 5′−3′ exonuclease Exo1 (Figure 3C). Remarkably, these exonucleases and polymerases with exonuclease activity show a reduced activity between 6 and 11% of that of *E. coli* ε (Figure 3D). This is, however, in agreement with previous literature.[2,32−34] Furthermore, exonuclease activity could also be readily measured for the commercially available *E. coli* exonuclease I and exonuclease III (Figure S7).

In the assay conditions used above (0.5 nM protein, 0.5 μM DNA), most curves exit the linear phase at ∼10 min, which is a reaction time that is too short when screening large compound libraries where several automated steps need to be executed sequentially for a large number of plates. Therefore, to slow down the reaction, we searched for an alternative way to influence the reaction velocity, as the protein concentration was already low (0.5 nM), and the DNA concentration was a 1000-fold higher (500 nM). Previously, using a gel-based exonuclease assay, we observed that the excision of a 3′

https://doi.org/10.1021/acsomega.2c06577
ACS Omega 2023, 8, 8285−8292

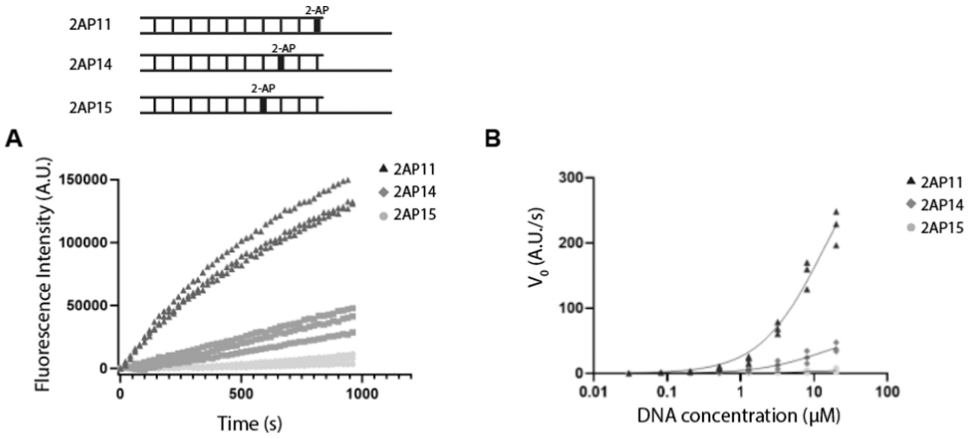

Figure 4. Position of 2-AP affects exonuclease activity. (A) Comparison of *E. coli* ε exonuclease activity using DNA substrates with the 2-AP at three different positions (highlighted in bold). Assay performed using 20 μM of each substrate and 0.5 nM of ε exonuclease. Data from three independent experiments (B) Graph showing initial slope velocity (V_0) of reactions performed using 1 nM of ε and increasing DNA concentration (0.08−20 μM). Data from three independent experiments.

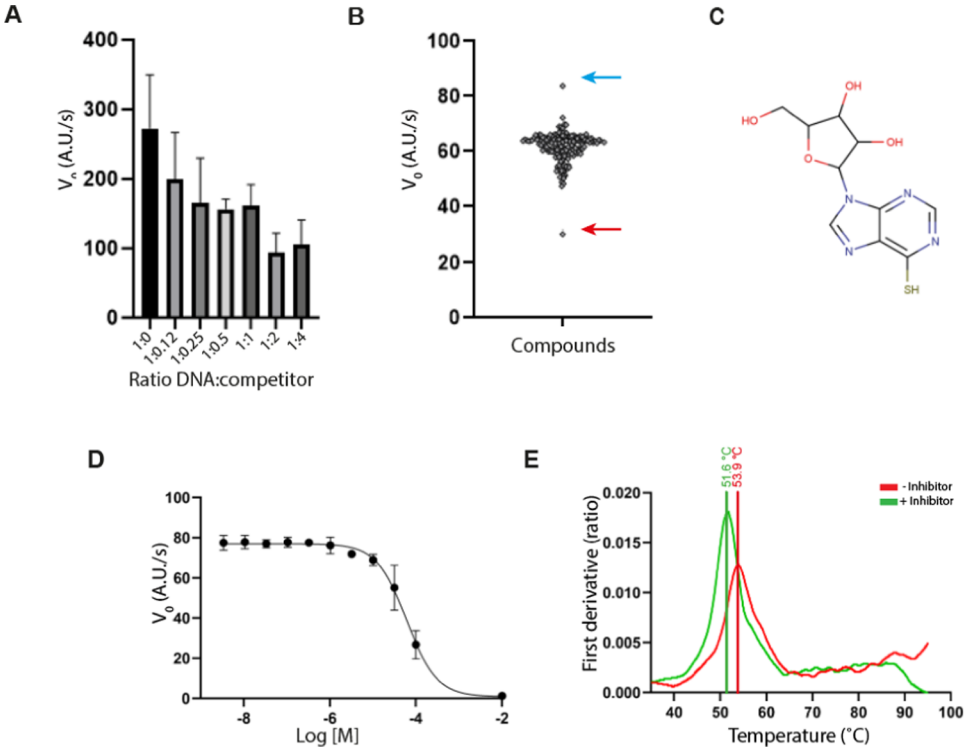

Figure 5. High-throughput screening using the 2-AP exonuclease assay (A) Initial slope velocities (V_0) for a 2-AP assay performed using 15 nM of *M. tuberculosis* DnaE1 and 1 μM of 2AP14 substrate and 0.12−4 μM of inhibitor DNA. (B) Violin plot showing the initial velocity values for each assay reaction in the respective wells. Values of V_0 around 65 indicate that there is no inhibition of protein activity. The red arrow indicates the hit compound 6-thioinosine. The blue arrow indicates a compound that shows intrinsic fluorescence. (C) Chemical structure of 6-thioinosine. (D) Dose−response curve of 6-thioinosine's inhibitory action on *M. tuberculosis* DnaE1 exonuclease activity. (E) First derivate plot of a thermal melt measurement of *M. tuberculosis* DnaE1 in the absence (red line) and presence (green line) of 6-thioinosine. Raw data in Figure S9B.

terminal 2-AP nucleotide was faster than a regular nucleotide (Figure S8). This faster excision of the 2-AP may be problematic when searching for potential exonuclease inhibitors, as weak inhibitors of "normal" exonuclease activity may not be effective on the faster 2-AP, and therefore will not be picked up during the screening of a chemical library. We therefore wondered if placing the 2-AP further away from the 3′ end could slow down the reaction, as the exonuclease would first have to remove regular nucleotides before excising the 2-AP (Figure 4A). Indeed, moving the 2-AP two or three nucleotides away from the 3′ end resulted in an ∼10 to 60-fold decrease of the exonuclease activity, respectively (Figure 4A,B). We therefore choose the DNA substrate with the 2-AP positioned two nucleotides away from the 3′ end (i.e., 2AP14) for all further experiments.

High-Throughput Inhibitor Screening Adaptability. Finally, to test the suitability of the 2-AP exonuclease as a high-throughput inhibitor screening tool, we chose the PHP-exonuclease domain of the replicate DNA polymerase DnaE1 from *M. tuberculosis* as a target for our inhibitor screen. The

https://doi.org/10.1021/acsomega.2c06577
ACS Omega 2023, 8, 8285−8292

PHP-exonuclease domain of DnaE1 is an attractive target for novel antibiotics, as it is biochemically and structurally distinct from the human exonucleases[35] and essential for viability in *M. tuberculosis*.[36] As the exonuclease activity of *M. tuberculosis* DnaE1 is lower than that of *E. coli* ε (Figure 3D), we increased the protein concentration from 0.5 to 15 nM to create an assay speed that is suitable for our high-throughput inhibitor screen setup. In addition, we used a Mantis (Formulatrix) automated liquid handling robot for rapid dispensing and reduction of the reaction volume from 15 to 10 μL. Under these conditions, we find that the mean fluorescence intensity signal in the presence of enzyme is $243.8 \times 10^3 \pm 6.7 \times 10^3$, while the background fluorescence intensity signal in the absence of enzyme is $78.2 \times 10^3 \pm 6.3 \times 10^3$, a 3-fold difference between the signal and background. This yields a *Z*-score of 0.8, which, together with other quality indicators (Figure S4), indicates a highly reliable confidence level[37] for the 2-AP exonuclease assay. In addition, we also tested a positive control for inhibition of exonuclease activity. For this, we used a DNA substrate that contains a slowly hydrolyzable phosphorothioate bond between the 3′ terminal nucleotide and adjacent nucleotide, which acts as a competitive inhibitor to the 2-AP substrate (Figure 5A and substrate ssDNA-P in Table S1). Already, at a concentration that is 10-fold less than the substrate DNA, the phosphorothioate DNA reduces the exonuclease activity by ∼30%, indicating that it is a suitable positive control for exonuclease inhibition.

Finally, to screen for potential inhibitors of the *M. tuberculosis* DnaE1 exonuclease, we used a nucleotide compound library from MedChemExpress that contains ∼200 nucleotide and nucleoside analogues. Using this library, we were able to identify a single hit compound, 6-thioinosine, which inhibits the exonuclease activity of *M. tuberculosis* DnaE1 by ∼50% at a 100 μM concentration (Figure 5B,C). The compound was further characterized by a dose−response curve (Figure 5D), yielding an IC_{50} of 64 μM. Binding of the 6-thioinosine to DnaE1 was also validated using differential scanning fluorometry that revealed a two-degree shift in the melting temperature of the protein (Figures 5E and S9). While the affinity of 64 μM is too low for a suitable drug candidate, it provides an attractive starting point for the development of better inhibitors against the exonuclease site of DnaE1 from *M. tuberculosis*. Finally, it is worth mentioning that some compounds show intrinsic fluorescence and may obscure the signal (Figure 5B). It is therefore helpful to also screen the compound library in the absence of enzyme to identify any intrinsically fluorescent candidates that need to be excluded from the results.

DISCUSSION AND CONCLUDING REMARKS

As the threat of drug-resistant and multi-drug-resistant bacteria is increasing worldwide,[38] the need for novel antibiotics with new modes of action is higher than ever. While inhibition of genome replication is frequently used in antiviral therapies, there are currently no antibiotics that directly target DNA replication in bacteria. Several inhibitors against bacterial replication proteins have been described, such as the *E. coli* DNA helicase DnaB, the sliding clamp β, the RNA primase DnaG, and the replicative DNA polymerases Pol C and DnaE,[39−41] yet there are currently none that have been developed into an antibiotic that is approved for use by the general public. Therefore, the need for novel DNA replication inhibitors remains. Replicative exonucleases are attractive targets for novel antibiotics, as disruption of exonuclease activity dramatically compromises viability in *E. coli*, *Salmonella typhimurium*, and *M. tuberculosis*.[28,29,36] Moreover, the majority of bacteria employ a so-called PHP-exonuclease[36] that is only found in bacteria and has no known homologues in eukaryotes,[42] thus reducing the likelihood of cross-species inhibition.

Exonucleases are also of interest as potential targets of anticancer drugs. More than 10 exo- and endonucleases are active in different forms of mammalian DNA repair (reviewed in ref 43). Furthermore, upregulation of EXO1 is associated with increased malignancies and correlated with a poor prognosis,[44,45] whereas the inhibition of APE2 has shown to reduce growth and malignancies.[46,47] Finally, ExoN, the replicative exonuclease of the SARS-CoV-2 virus, is also the target of novel promising antiviral drugs.[48]

To aid in the search for novel exonuclease inhibitors, we have developed a simple and versatile exonuclease assay that can be used for both 3′−5′ and 5′−3′ exonucleases, as well as bacterial and human exonucleases. Using this assay that is compatible with high-throughput inhibitor screening, we have discovered a novel inhibitor of the *M. tuberculosis* DnaE1 exonuclease that is essential for viability in this bacterium. Hence, our work describes a novel, real-time exonuclease assay that can be used to search for novel inhibitors of DNA replication of DNA repair. Given that 2-AP has also been used for the study of other DNA-modifying enzymes such as those involved in DNA repair and DNA modification, we envision that similar real-time high-throughput assays could also be developed for these enzymes and aid in the search for new inhibitors that in turn may be developed into novel therapies.

ASSOCIATED CONTENT

Supporting Information

The Supporting Information is available free of charge at https://pubs.acs.org/doi/10.1021/acsomega.2c06577.

Additional biochemical characterization of different exonucleases and substrates, composition of DNA substrates, composition of buffer screen, and composition of nucleotide analogue library (PDF)

Accession Codes

Accession codes for proteins used in this study: *E. coli* DNA polymerase III α, P10443; *E. coli* DNA polymerase III ε, P03007; *E. coli* DNA polymerase I, P00582; *M. tuberculosis* DnaE1, P9WNT7; human DNA polymerase δ catalytic subunit, P28340; human EXO1, Q9UQ84.

AUTHOR INFORMATION

Corresponding Author

Meindert H. Lamers − *Cell and Chemical Biology Department, Leiden University Medical Center, 2333 ZC Leiden, The Netherlands*; orcid.org/0000-0002-4205-1338; Email: m.h.lamers@lumc.nl

Authors

Margherita M. Botto − *Cell and Chemical Biology Department, Leiden University Medical Center, 2333 ZC Leiden, The Netherlands*

Sudarshan Murthy − *Cell and Chemical Biology Department, Leiden University Medical Center, 2333 ZC Leiden, The Netherlands*

Complete contact information is available at:

https://doi.org/10.1021/acsomega.2c06577
ACS Omega 2023, 8, 8285−8292

https://pubs.acs.org/10.1021/acsomega.2c06577

Author Contributions

The manuscript was written through contributions of all authors. All authors have given approval to the final version of the manuscript.

Notes

The authors declare no competing financial interest.

■ ACKNOWLEDGMENTS

Pol δ was a kind gift from the laboratory of Prof. Hamdan at King Abdullah University of Science and Technology, Saudi Arabia. This work was supported by a LUMC Research Fellowship to M.H.L.

■ REFERENCES

(1) Mason, P. A.; Cox, L. S. The Role of DNA Exonucleases in Protecting Genome Stability and Their Impact on Ageing. *Age* **2012**, *34*, 1317−1340.
(2) Nasir, N.; Kisker, C. Mechanistic Insights into the Enzymatic Activity and Inhibition of the Replicative Polymerase Exonuclease Domain from Mycobacterium Tuberculosis. *DNA Repair* **2019**, *74*, 17−25.
(3) Standish, A. J.; Salim, A. A.; Capon, R. J.; Morona, R. Dual Inhibition of DNA Polymerase PolC and Protein Tyrosine Phosphatase CpsB Uncovers a Novel Antibiotic Target. *Biochem. Biophys. Res. Commun.* **2013**, *430*, 167−172.
(4) Hamdan, S.; Bulloch, E. M.; Thompson, P. R.; Beck, J. L.; Yang, J. Y.; Crowther, J. A.; Lilley, P. E.; Carr, P. D.; Ollis, D. L.; Brown, S. E.; Dixon, N. E. Hydrolysis of the 5′-p-Nitrophenyl Ester of TMP by the Proofreading Exonuclease (ε) Subunit of Escherichia Coli DNA Polymerase III. *Biochemistry* **2002**, *41*, 5266−5275.
(5) Matsuura, S. I.; Komatsu, J.; Hirano, K.; Yasuda, H.; Takashima, K.; Katsura, S.; Mizuno, A. Real-Time Observation of a Single DNA Digestion by λ Exonuclease under a Fluorescence Microscope Field. *Nucleic Acids Res.* **2001**, *29*, e79.
(6) Mason, P. A.; Boubriak, I.; Cox, L. S. A Fluorescence-Based Exonuclease Assay to Characterize DmWRNexo, Orthologue of Human Progeroid WRN Exonuclease, and Its Application to Other Nucleases. *J. Vis. Exp.* **2013**, *82*, e50722.
(7) Buzon, B.; Grainger, R. A.; Rzadki, C.; Huang, S. Y. M.; Junop, M. Identification of Bioactive SNM1A Inhibitors. *ACS Omega* **2021**, *6*, 9352−9361.
(8) Ronen, A. 2-Aminopurine. *Mutat. Res.* **1979**, *75*, 1−47.
(9) Jean, J. M.; Hall, K. B. 2-Aminopurine Fluorescence Quenching and Lifetimes: Role of Base Stacking. *Proc. Natl. Acad. Sci. U.S.A.* **2001**, *98*, 37−41.
(10) Li, X.; Yang, H.; He, J.; Yang, B.; Zhao, Y.; Wu, P. Full Liberation of 2-Aminopurine with Nucleases Digestion for Highly Sensitive Biosensing. *Biosens. Bioelectron.* **2022**, *196*, No. 113721.
(11) Sowers, L. C.; Fazakerley, G. V.; Eritja, R.; Kaplan, B. E.; Goodman, M. F. Base Pairing and Mutagenesis: Observation of a Protonated Base Pair between 2-Aminopurine and Cytosine in an Oligonucleotide by Proton NMR. *Proc. Natl. Acad. Sci. U.S.A.* **1986**, *83*, 5434−5438.
(12) Law, S. M.; Eritja, R.; Goodman, M. F.; Breslauer, K. J. Spectroscopic and Calorimetric Characterizations of DNA Duplexes Containing 2-Aminopurine. *Biochemistry* **1996**, *35*, 12329−12337.
(13) Fagan, P. A.; Fàbrega, C.; Eritja, R.; Goodman, M. F.; Wemmer, D. E. NMR Study of the Conformation of the 2-Aminopurine:Cytosine Mismatch in DNA. *Biochemistry* **1996**, *35*, 4026−4033.
(14) Stivers, J. T. 2-Aminopurine Fluorescence Studies of Base Stacking Interactions at Abasic Sites in DNA: Metal-Ion and Base Sequence Effects. *Nucleic Acids Res.* **1998**, *26*, 3837−3844.
(15) Guest, C. R.; Hochstrasser, R. A.; Sowers, L. C.; Millar, D. P. Dynamics of Mismatched Base Pairs in DNA. *Biochemistry* **1991**, *30*, 3271−3279.
(16) Moe, J. G.; Russu, I. M. Kinetics and Energetics of Base-Pair Opening in 5′;-d(CGCGAATTCGCG)-3′ and a Substituted Dodecamer Containing G•T Mismatches. *Biochemistry* **1992**, *31*, 8421−8428.
(17) Nordlund, T. M.; Xu, D.; Evans, K. O. Excitation Energy Transfer in DNA: Duplex Melting and Transfer from Normal Bases to 2-Aminopurine. *Biochemistry* **1993**, *32*, 12090−12095.
(18) Bloom, L. B.; Goodman, M. F.; Otto, M. R.; Beechem, J. M.; Eritja, R.; Reha-Krantz, L. J. Pre-Steady-State Kinetic Analysis of Sequence-Dependent Nucleotide Excision by the 3′-Exonuclease Activity of Bacteriophage T4 DNA Polymerase. *Biochemistry* **1994**, *33*, 7576−7586.
(19) Frey, M. W.; Sowers, L. C.; Millar, D. P.; Benkovic, S. J. The Nucleotide Analog 2-Aminopurine as a Spectroscopic Probe of Nucleotide Incorporation by the Klenow Fragment of Escherichia Coli Polymerase I and Bacteriophage T4 DNA Polymerase. *Biochemistry* **1995**, *34*, 9185−9192.
(20) Teklemariam, T. A.; Rivera, O. D.; Nelson, S. W. Kinetic Analysis of the Exonuclease Activity of the Bacteriophage T4 MRE11−Rad50 Complex. *Methods Enzymol.* **2018**, *600*, 135−156.
(21) Allan, B. W.; Reich, N. O. Targeted Base Stacking Disruption by the EcoRI DNA Methyltransferase. *Biochemistry* **1996**, *35*, 14757−14762.
(22) Bonnist, E. Y. M.; Liebert, K.; Dryden, D. T. F.; Jeltsch, A.; Jones, A. C. Using the Fluorescence Decay of 2-Aminopurine to Investigate Conformational Change in the Recognition Sequence of the EcoRV DNA-(Adenine-N6)- Methyltransferase on Enzyme Binding. *Biophys. Chem.* **2012**, *160*, 28−34.
(23) Jones, A. C.; Neely, R. K. 2-Aminopurine as a Fluorescent Probe of DNA Conformation and the DNA-Enzyme Interface. *Q. Rev. Biophys.* **2015**, *48*, 244−279.
(24) Rachofsky, E. L.; Osman, R.; Ross, J. B. A. Probing Structure and Dynamics of DNA with 2-Aminopurine: Effects of Local Environment on Fluorescence. *Biochemistry* **2001**, *40*, 946−956.
(25) Shi, Y.; Hellinga, H. W.; Beese, L. S. Interplay of Catalysis, Fidelity, Threading, and Processivity in the Exo-and Endonucleolytic Reactions of Human Exonuclease i. *Proc. Natl. Acad. Sci. U.S.A.* **2017**, *114*, 6010−6015.
(26) Lehman, I. R.; Nussbaum, A. L. The Deoxyribonucleases of Escherichia Coli. *J. Biol. Chem.* **1964**, *239*, 2628−2636.
(27) Scheuermann, R.; Tam, S.; Burgers, P. M. J. Identification of the ε-Subunit of Escherichia Coli DNA Polymerase III Holoenzyme as the DnaQ Gene Product: A Fidelity Subunit for DNA Replication. *Proc. Natl. Acad. Sci. U.S.A.* **1983**, *80*, 7085−7089.
(28) Scheuermann, R. H.; Echols, H. A Separate Editing Exonuclease for DNA Replication: The ε Subunit of Escherichia Coli DNA Polymerase III Holoenzyme. *Proc. Natl. Acad. Sci. U.S.A.* **1984**, *81*, 7747−7751.
(29) Lancy, E. D.; Lifsics, M. R.; Kehres, D. G.; Maurer, R. Isolation and Characterization of Mutants with Deletions in DnaQ, the Gene for the Editing Subunit of DNA Polymerase III in Salmonella Typhimurium. *J. Bacteriol.* **1989**, *171*, 5572−5580.
(30) Zhang, Z. W. PH-Sensitive Fluorescent Dyes: Are They Really PH-Sensitives in Cells? *Mol. Pharmaceutics* **2013**, *239*, 1910−1917.
(31) Dodd, T.; Botto, M.; Paul, F.; Fernandez-Leiro, R.; Lamers, M. H.; Ivanov, I. Polymerization and Editing Modes of a High-Fidelity DNA Polymerase Are Linked by a Well-Defined Path. *Nat. Commun.* **2020**, *11*, No. 5379.
(32) Miller, H.; Perrino, F. W. Kinetic Mechanism of the 3′ → 5′ Proofreading Exonuclease of DNA Polymerase III. Analysis by Steady State and Pre-Steady State Methods. *Biochemistry* **1996**, *35*, 12919−12925.
(33) Eger, B. T.; Carroll, S. S.; Benkovic, P. A.; Dahlberg, M. E.; Benkovic, S. J.; Kuchta, R. D.; Joyce, C. M. Mechanism of DNA Replication Fidelity for Three Mutants of DNA Polymerase I: Klenow

Fragment KF(Exo+), KF(PolA5), and KF(Exo−). *Biochemistry* **1991**, *30*, 1441−1448.
(34) Meng, X.; et al. The P12 Subunit of Human Polymerase Delta Modulates the Rate and Fidelity of DNA Synthesis. *Biochemistry* **2013**, *17*, 3545−3554.
(35) Baños-Mateos, S.; Roon, A. M.; Lang, U. F.; Maslen, S. L.; Skehel, J. M.; Lamers, M. H. High-Fidelity DNA Replication in Mycobacterium Tuberculosis Relies on a Trinuclear Zinc Center. *Nat. Commun.* **2017**, *8*, No. 855.
(36) Rock, J. M.; Lang, U. F.; Chase, M. R.; Ford, C. B.; Gerrick, E. R.; Gawande, R.; Coscolla, M.; Gagneux, S.; Fortune, S. M.; Lamers, M. H. DNA Replication Fidelity in Mycobacterium Tuberculosis Is Mediated by an Ancestral Prokaryotic Proofreader. *Nat. Genet.* **2015**, *47*, 677−681.
(37) Zhang, J.-H.; Chung, T. D. Y.; Oldenburg, K. R. A Simple Statistical Parameter for Use in Evaluation and Validation of High Throughput Screening Assays. *J. Biomol. Screen.* **1999**, *4*, 67−73.
(38) Murray, C. J.; Ikuta, K. S.; Sharara, F.; Swetschinski, L.; Robles Aguilar, G.; Gray, A.; Han, C.; Bisignano, C.; Rao, P.; Wool, E.; Johnson, S. C.; et al. Global Burden of Bacterial Antimicrobial Resistance in 2019: A Systematic Analysis. *Lancet* **2022**, *399*, 629−655.
(39) Reiche, M. A.; Warner, D. F.; Mizrahi, V. Targeting DNA Replication and Repair for the Development of Novel Therapeutics against Tuberculosis. *Front. Mol. Biosci.* **2017**, *4*, 75.
(40) Robinson, A.; J Causer, R.; E Dixon, N. Architecture and Conservation of the Bacterial DNA Replication Machinery, an Underexploited Drug Target. *Curr. Drug Targets* **2012**, *13*, 352−372.
(41) Kaguni, J. M. The Macromolecular Machines That Duplicate the Escherichia Coli Chromosome as Targets for Drug Discovery. *Antibiotics* **2018**, *7*, 23.
(42) Aravind, L.; Koonin, E. V. Phosphoesterase Domains Associated with DNA Polymerases of Diverse Origins. *Nucleic Acids Res.* **1998**, *26*, 3746−3752.
(43) Manils, J.; Marruecos, L.; Soler, C. Exonucleases: Degrading DNA to Deal with Genome Damage, Cell Death, Inflammation and Cancer. *Cells* **2022**, *11*, 2157.
(44) Mao, P.; Wu, S.; Fan, Y. Upregulation of Exonuclease 1 Caused by Homology-Dependent Repair Confers Cisplatin Resistance to Gastric Cancer Cells. *Can. J. Physiol. Pharmacol.* **2022**, *100*, No. e139.
(45) Liu, J.; Zhang, J. Elevated EXO1 Expression Is Associated with Breast Carcinogenesis and Poor Prognosis. *Ann. Transl. Med.* **2021**, *9*, 135.
(46) Omkar, S.; Wani, T. H.; Zheng, B.; Mitchem, M. M.; Truman, A. W. The APE2 Exonuclease Is a Client of the Hsp70-Hsp90 Axis in Yeast and Mammalian Cells. *Biomolecules* **2022**, *12*, No. 864.
(47) Hossain, M. A.; Lin, Y.; Driscoll, G.; Li, J.; McMahon, A.; Matos, J.; Zhao, H.; Tsuchimoto, D.; Nakabeppu, Y.; Zhao, J.; Yan, S. APE2 Is a General Regulator of the ATR-Chk1 DNA Damage Response Pathway to Maintain Genome Integrity in Pancreatic Cancer Cells. *Front. Cell Dev. Biol.* **2021**, *9*, 738502.
(48) Wang, X.; Tao, C.; Morozova, I.; Kalachikov, S.; Li, X.; Kumar, S.; Russo, J. J.; Ju, J. Identifying Structural Features of Nucleotide Analogues to Overcome SARS-CoV-2 Exonuclease Activity. *Viruses* **2022**, *14*, No. 1413.

https://doi.org/10.1021/acsomega.2c06577
ACS Omega 2023, 8, 8285−8292